FRACTURE PROPERTIES AND TOUGHENING MECHANISMS OF CTBN RUBBER MODIFIED EPOXY SYNTACTIC FOAMS

Sammy He[1], Declan Carolan[1,2], Alexander Fergusson[1,2] and Ambrose C. Taylor[2]

[1] FAC Technology, 53 Lydden Grove, Wandsworth, London SW18 4LW, UK
Email: sammy@factechnology.com (S. He), declan@factechnology.com (D. Carolan), alex@factechnology.com (A. Fergusson)

[2] Department of Mechanical Engineering, Imperial College London, London SW7 2AZ, UK
Email: a.c.taylor@imperial.ac.uk (A. C. Taylor)
Webpage: http://www.imperial.ac.uk/people/a.c.taylor (A. C. Taylor)

Keywords: syntactic foam, CTBN rubber, fracture, toughening mechanisms

ABSTRACT

Syntactic foams, utilised in aerospace and naval industries for their lightweight and high specific strength, suffer from brittleness. This study aimed to improve fracture toughness by modifying the epoxy polymer matrix in an epoxy/hollow glass microsphere (GMS) syntactic foam with carboxyl-terminated butadiene-acrylonitrile (CTBN) rubber. The microstructure and fracture properties were compared to CTBN-modified bulk epoxy polymers. While CTBN incorporation led to complex microstructures and increased fracture energy in the foam (from 193 J/m^2 to 296 J/m^2 at 12 wt% CTBN concentration), the improvement was smaller compared to bulk epoxy polymers (101 J/m^2 to 1112 J/m^2 for the same CTBN concentration). Limited toughness transfer was attributed to the small interstitial regions between GMS, restricting the plastic zone size. Nevertheless, the achieved increase in fracture energy in this research has the potential to enhance the overall applicability of syntactic foams in structural uses.

1 INTRODUCTION

The brittle nature of syntactic foams, which are based on highly crosslinked thermosetting polymers, limits their applications. Previous studies have focused on enhancing the mechanical and fracture properties of syntactic foams by incorporating reinforcing particles like nanoclay [1, 2], graphene platelets [3, 4], carbon nanofibres [5, 6], and high aspect ratio microfibres [7–9]. These attempts have yielded varying degrees of success, with improvements ranging from 25% to 180% compared to the base material. However, there has been limited exploration of directly modifying the epoxy matrix to enhance fracture toughness. For bulk epoxy polymers in structural applications, toughening is necessary to resist defect growth and subsequent failure, typically achieved by introducing a second phase into the material. One commonly used method involves incorporating rubbery particles, such as carboxyl-terminated butadiene-acrylonitrile (CTBN), which were first utilized in the 1970s [10]. These rubbery particles are usually pre-dissolved in the epoxy resin and phase separate during the curing process, forming micron-sized rubber particles. The evolution of the rubbery phase in the epoxy can be described by the Cahn-Hilliard equation [11, 12], which depends on the rubber concentration and mixture mobility, governing the size and morphology of the phase-separated rubber particles. Numerous studies have reported significant increases in fracture toughness with the addition of CTBN in epoxy polymers [13], attributing the main toughening mechanisms to shear band yielding, rubber particle cavitation, and subsequent matrix void growth. Analytical modeling of these toughening mechanisms has been well-established. However, the extent to which these toughness enhancements can be transferred to syntactic foams when CTBN-modified epoxy is used as the matrix remains poorly understood.

To overcome the brittleness of syntactic foams, this study investigates the effect of using CTBN rubber as a toughening modifier in bulk epoxy polymers, and in the epoxy matrix of syntactic foams. The morphologies of the CTBN rubber particles are compared for the two material types, and the differences

are explained in terms of curing kinetics and preferential surface adsorption. The fracture properties were also measured and compared, particularly to assess how effectively the increased fracture properties were transferred from the bulk material to the syntactic foam. Scanning electron microscopy was then used to identify the toughening mechanisms involved.

2 EXPERIMENTAL

2.1 Materials and manufacturing

Plates of bulk epoxy polymer and syntactic foam were manufactured such that comparison of the morphology, mechanical and fracture properties, and toughening mechanisms of the two materials could be made. The epoxy resin was a standard diglycidyl ether of bisphenol-A (DGEBA), 'Araldite LY556', with an epoxide equivalent weight (EEW) of 185 g/eq. The curing agent was a methyltetrahydrophthalic anhydride, 'Aradur HY917', with an anhydride equivalent weight (AHEW) of 166 g/eq. An accelerator in the form of a heterocyclic amine catalyst, 1-methylimidazole, 'Accelerator DY070', was also used. All epoxy components were supplied by Huntsman, UK. The epoxy, curing agent, and accelerator were used at a stoichiometric ratio of 100:90:1, respectively.

Carboxyl-terminated butadiene-acrylonitrile (CTBN) reactive liquid rubber was used as a toughening agent for the epoxy polymer. The CTBN rubber was supplied as an adduct, pre-reacted and dissolved in DGEBA resin as 'Albipox 1000', by Evonik, Germany. This has an EEW of 330 g/eq [14], and has 40 weight percentage (wt%) CTBN rubber content. To prepare the bulk epoxy material, the required concentration of CTBN rubber was obtained by diluting the masterbatch with additional DGEBA, 'Araldite LY556'. A stoichiometric amount of the anhydride curing agent and accelerator were added, and was stirred thoroughly and then degassed in a vacuum oven at 60 °C and -1 atm, until no additional air bubbles were formed. This was then poured into release-coated steel vertical moulds of thicknesses 3 mm and 6 mm. The epoxy was cured at in an oven at 80 °C for 4 hours, followed by a post-cure at 140 °C for 8 hours, as recommended by Huntsman [15]. Bulk epoxy polymer plates with up to 12 wt% CTBN were manufactured. In the literature, 9 wt% of CTBN is typically the optimum concentration in terms of achieving the greatest fracture toughness [16–18].

Borosilicate hollow glass microspheres (GMS) of type 'S38' from 3M, UK, were used to manufacture the syntactic foams. These microspheres have a mean diameter of 40 μm, a mean wall thickness of 1.28 μm with no porosity, a true density of 380 kg/m^3, a crush strength of 27.6 MPa (for 90% survival), and no surface treatment [19]. The syntactic foams were manufactured so that the GMS are densely packed, up to a packing factor of approximately 60%, according to the product data sheet [19]. This is to maximise the hollow content provided by the GMS, thus reducing density and weight which is desirable in the weight-sensitive applications in which syntactic foams are commonly used. This packing factor was confirmed in a previous study [7], where a volume fraction of 60.7% was measured by performing volume fraction analysis on optical microscopy images of the syntactic foam cross-sections. The CTBN modified epoxy polymer matrix was prepared using the same method described above for the bulk material. Epoxy polymer matrices with up to 12 wt% CTBN rubber were used. The GMS are embedded into the epoxy matrix and the plates of syntactic foam were manufactured in a mould, and were subject to the same curing cycle as the bulk epoxy polymer. The plates produced were then milled to a thickness of 8 mm using a TM-2 CNC machine from Haas, UK.

2.2 Mechanical testing

The fracture energy, G_{IC}, was determined using single edge notch bending (SENB) tests in accordance with ISO 13586 [20] using specimens of dimensions $80 \times 16 \times 8$ mm^3. A V-notch was machined at the mid-length using a horizontal mill to a depth of 5.3 mm. A liquid nitrogen cooled razor blade was then carefully tapped into the V-notch to produce a sharp pre-crack before testing. The specimens were tested at room temperature at a displacement rate of 1 mm/min using an Instron 3366 universal testing machine fitted with a 10 kN load cell. At least ten valid tests were performed for each formulation.

2.3 Image analysis

The morphology of the bulk epoxy polymers was determined using atomic force microscopy (AFM). A scanning probe microscope, 'MultiMode 8', equipped with an 'E' scanner and controlled by a NanoScope IV controller (from Veeco, USA) was used. Flat and smooth surfaces were cut on the samples using a ultramicrotome, 'PowerTome XL', from RMC Products, USA. The ultramicrotome was operated at room temperature. Phase images of resolution 512 $\times$ 512 pixels at scan sizes of 20 $\times$ 20 μm^2 and 50 $\times$ 50 μm^2 were obtained using silicon probes, operated in tapping mode at a scan speed of 1 Hz. Soft material will appear darker in the phase images so that the CTBN rubber can be readily identified.

A Hitachi S-3400N scanning electron microscope (SEM) was used to observe the fracture surfaces of the SENB samples to identify the toughening mechanisms. The samples were mounted on aluminium stubs and sputter-coated with a 10 nm thick layer of gold to minimise charging. An accelerating voltage of 10 kV was used.

3 RESULTS & DISCUSSION

3.1 Microstructure

3.1.1 Bulk epoxy polymer

The morphology of the CTBN modified bulk epoxy polymers was determined using atomic force microscopy (AFM), and selected phase micrographs are shown in Figure 1. The CTBN rubber particles are identified as dark regions in the phase images since they have a much lower stiffness compared to the epoxy. These micrographs are an illustrative, typical representation of the CTBN particles before fracture, hence the initial particle radius can be measured. This is then compared to the radius of the voids on the fracture surface, which will indicate whether the plastic void growth toughening mechanism has occurred, as discussed later in

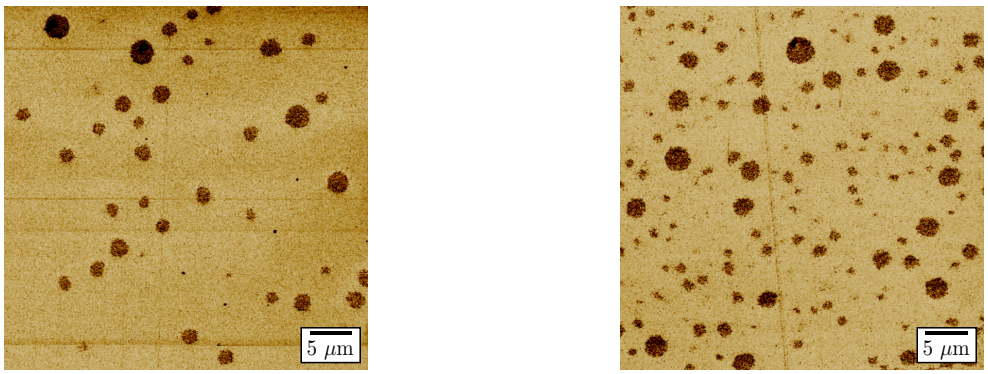

(a) 6 wt% CTBN (b) 9 wt% CTBN

Figure 1: AFM phase micrographs of CTBN rubber modified bulk epoxy polymers.

The dark circular features on the AFM images show that the CTBN rubber has phase separated into well-dispersed spherical particles within the bulk epoxy. By inspection of the AFM micrographs, the distribution of rubber particle sizes is assumed to be the same for all CTBN concentrations. This has been observed by Kinloch and Hunston [21], where no significant differences in mean particle radius were measured in a similar range of CTBN concentrations. The radii of the CTBN particles were measured and a mean value of 0.87 $\pm$ 0.38 μm was obtained. This value is the corrected value which takes into account the microtoming process, using well-known stereological methods [22].

3.1.2 Syntactic foam

It was not possible to use atomic force microscopy to determine the morphology of the CTBN rubber in the syntactic foam, due to the large size of the GMS relative to the scanning area of the AFM. The morphology of the CTBN rubber in the epoxy matrix of the syntactic foam was inferred from SEM images of the fracture surfaces, which are shown in Figure 2. The images confirm that CTBN rubber was present in the interstitial spaces between the microspheres.

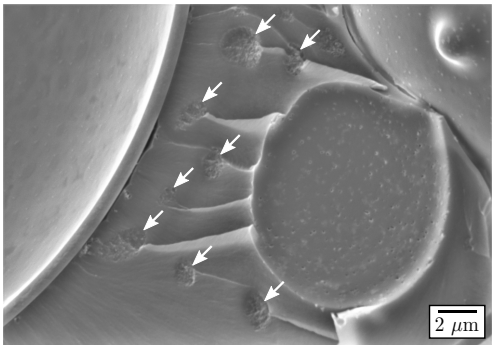

(a) 3 wt% CTBN

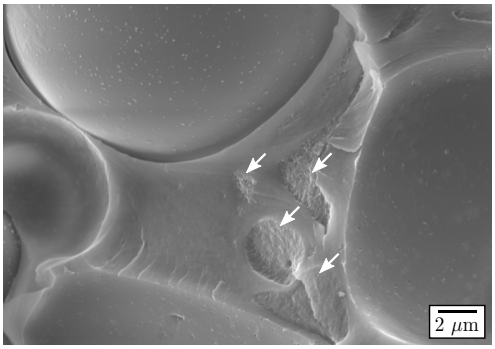

(b) 6 wt% CTBN

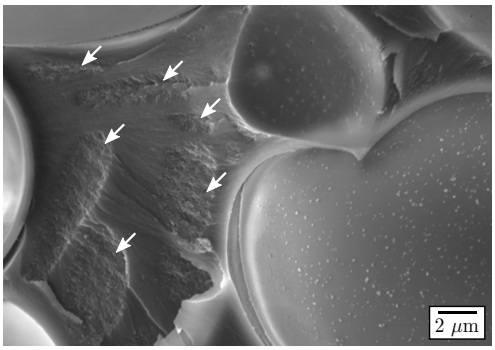

(c) 9 wt% CTBN

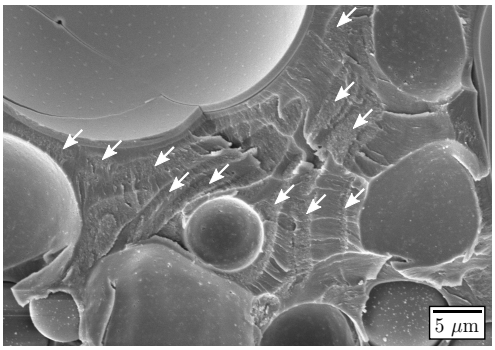

(d) 12 wt% CTBN

Figure 2: Scanning electron micrographs of the fracture surfaces of CTBN rubber modified syntactic foams. Rubber particles are indicated by arrows. Crack propagation direction is from left to right.

For the syntactic foams with 3 wt% CTBN modified epoxy, circular features such as those seen in Figure 2a suggest that the CTBN has phase separated into spherical particles. When the CTBN concentration increases to 6 wt%, some particles remain spherical, while some particles begin to elongate along the surface of the glass microspheres. The elongation increases with the 9 wt% CTBN modified syntactic foam, where rubber particles that have a characteristic length of up to 10 μm, such as those in Figure 2c, can be seen. These indicate that co-continuous structures of CTBN were formed. When the CTBN concentration is further increased to 12 wt%, lamellar structures of alternating CTBN and epoxy layers are seen, see Figure 2d. Phase inversion is also evident, where voids left by epoxy particles within rubber-rich regions of up to 10 μm in diameter are observed, see Figure 3. These voids have an average diameter of 2 μm and are much smaller than the GMS, so it can be inferred they were left by epoxy particles. Clearly, the presence of GMS has caused the CTBN to phase separate into a complex microstructure that is radically different to that seen for the bulk epoxy polymer, where all of the CTBN particles were spherical for all of the volume fractions of CTBN investigated.

3.1.3 Phase separation

The presence of co-continuous structures of rubber in the epoxy matrix of the syntactic foam indicates that the CTBN phase separated via the spinodal decomposition mechanism [23]. This is opposed to the nucleation and growth mechanism where only spherical morphologies are possible [24], although spinodal decomposition can also form spherical particles. Structures that are formed during phase separation are fixed in place as the epoxy reaches gelation. This is due to the viscosity of the resin increasing as crosslinks are established, and the molecular mobility is greatly restricted. The bulk epoxy polymer and syntactic foam are not likely to gel at significantly different times to cause a difference in rubber particle morphology, since the curing kinetics and glass transition temperatures (using differential scanning calorimetry (DSC) and dynamic mechanical thermal analysis tests (DMTA), respectively) of the two material types were determined to be very similar.
In a mixture containing a primary and secondary phase, the process that governs spinodal decomposition was proposed by Cahn and Hilliard [11], and is dependent on the mobility of the mixture, and the concentration of the secondary phase. At low concentration values of the secondary phase, spherical particle morphologies were formed, while at larger concentrations, co-continuous structures are promoted [25]. This mirrors what was seen in the syntactic foams; spherical particles at 3 wt% CTBN, and co-continuous structures at 9 wt% and above. However, this does not occur for the bulk epoxy polymers as only spherical particles were observed. The transition from spherical to co-continuous structures in bulk epoxy polymers has been observed to occur at much higher concentrations (about 25 wt%) [26, 27]. The difference in CTBN morphologies between the bulk epoxy polymer and syntactic foam was therefore compelling.

By observation of the SEM micrographs in Figure 2, the CTBN particles appear to elongate along the geometry of the GMS, and are also up to an order of magnitude larger than the CTBN particles in the bulk epoxy. This observation is similar to work by Wiltzius and Cumming [28, 29], who studied the influence of a quartz wall on the spinodal decomposition of a polyisoprene and poly(ethylene-propylene) blend. Using light-scattering, they observed that phase separated domains in the bulk away from the wall grew as an exponent of time that is proportional to $t^{1/3}$, which is typical with diffusion-driven dynamics (phase separation is a diffusion process [11]). However, the growth of the domains that were near the wall accelerated greatly, proportional to $t^{3/2}$, and these domains were also growing parallel to the surface. This behaviour could not be explained by diffusion- or interface-driven dynamics.

The authors attributed this behaviour to a wetting effect caused by one of the phases showing preferential adsorption to the quartz surface [29]. Adsorption is certainly present for the CTBN modified syntactic foams in this study. Epoxy molecules are preferentially adsorbed onto the surfaces of the GMS due to strong polar attractions between hydroxyl groups present on the epoxy molecules and the glass surfaces [30, 31]. This is supported by the SEM images, where the GMS appear to be only coated with epoxy and never CTBN, even at high CTBN concentrations. This is highlighted clearly in Figure 3 where the epoxy and CTBN phases are colourised in orange and dark blue, respectively. The epoxy therefore acts as the wetting component to the GMS surfaces.

Troian [32] developed this theory and proposed a mechanism for the increase in domain growth near a surface, as shown schematically in Figure 4. When the wetting component adheres to the wall, the diffusive growth of the non-wetting component is slowed in the direction perpendicular to the wall, and will instead grow laterally to compensate (Figure 4b). The wetting layer has therefore reduced the dimensionality of the diffusion process, as the 3D domains are now growing along a 2D surface.

By taking the radius of curvature of the non-wetting component at the surface to be much less than that in the bulk, Troian was able to prove that the diffusive growth due to the reduced dimensionality scales as $t^{1/2}$ (the full proof can be found in [32]). Further, the effect of particle coalescence (Figure 4c) can accelerate this growth [33, 34], to give the experimentally observed scaling of $t^{3/2}$ found by Wiltzius and Cumming [28, 29].

For the case of the syntactic foam, it is difficult to determine the precise growth evolution of the CTBN particles since the gelation time of the epoxy is unknown. However, Wiltzius and Cumming

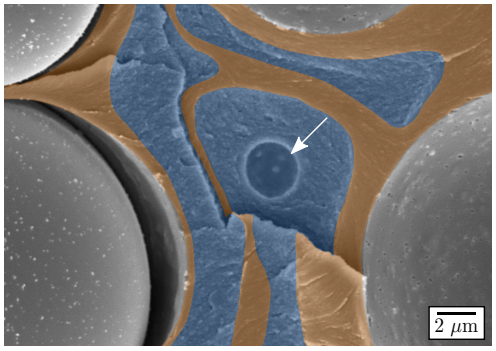

Figure 3: Scanning electron micrograph of the fracture surface of 12 wt% CTBN modified syntactic foam. Epoxy and CTBN phases are colourised in orange and dark blue, respectively. A void within a rubber-rich phase left by an epoxy particle is indicated with an arrow. Crack propagation direction is from left to right.

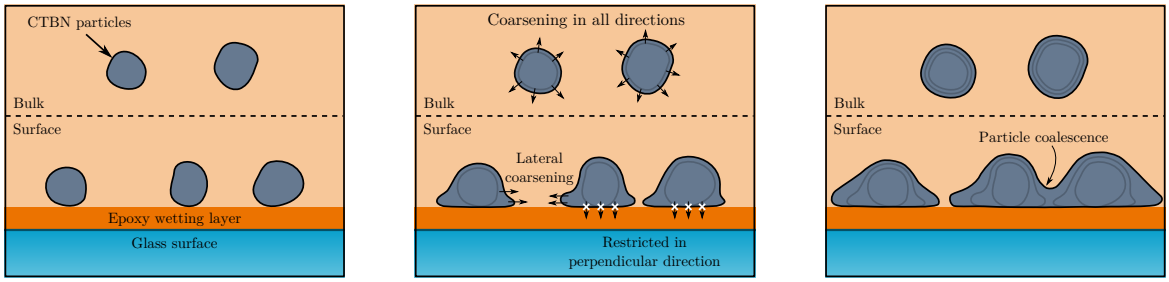

(a) (b) (c)

Figure 4: Schematic diagram of CTBN particle growth in the bulk and near a surface during spinodal decomposition [32].

observed the same $t^{1/3}$ and $t^{3/2}$ growth for the bulk and surface, respectively, regardless of quench depth [28, 29]. An example growth evolution of the CTBN particles is presented in Figure 5 for visual clarity. The radius of the CTBN particles is plotted against an arbitrary function of $t^{1/3}$ and $t^{3/2}$. After a given time before gelation (indicated by the dashed line in Figure 5), the length scales are comparable to what was observed in the SEM images of the CTBN modified bulk epoxy and syntactic foam. The difference in CTBN particle morphology was thus determined to be due to reduced dimensionality and particle coalescence introduced by the presence of the glass microspheres.

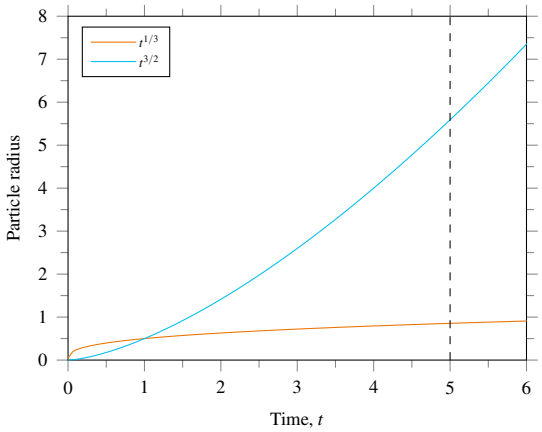

Figure 5: Particle radius versus time where radius is an arbitrary function of $t^{1/3}$ (representing phase separation in a typical diffusion process) and $t^{3/2}$ (representing phase separation with reduced dimensionality and particle coalescence). The dashed line represents the time of gelation.

3.2 Fracture properties

The fracture toughness, K_{IC}, and fracture energy, G_{IC}, of the CTBN modified bulk epoxy polymers and syntactic foams were determined using SENB tests. The results for the K_{IC} and G_{IC} values are shown in Figure 6. The K_{IC} of the bulk epoxy polymer increases with increasing CTBN concentration, from 0.63 ± 0.03 MPa $m^{1/2}$ for the unmodified epoxy, to 1.59 ± 0.05 MPa $m^{1/2}$ for the 12 wt% concentration. The G_{IC} follows the same trend, from 101 ± 8 J/m^2 for the unmodified epoxy, to 1112 ± 47 J/m^2 for 12 wt% CTBN, corresponding to a 1000% improvement in fracture energy. This large increase in fracture performance is expected of rubber modified epoxies [13], due to the shear band yielding and plastic void growth toughening mechanisms [35], both of which are evident in this study.

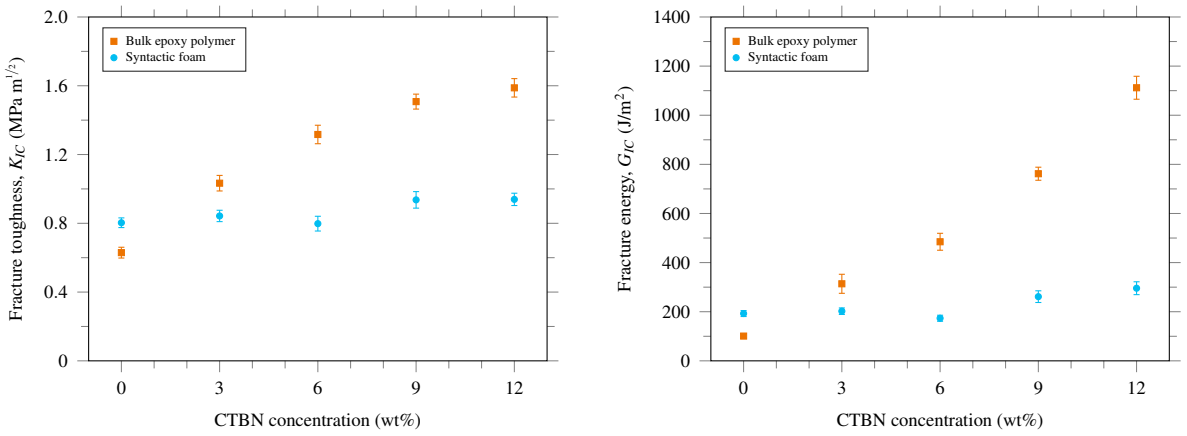

(a) Fracture toughness

(b) Fracture energy

Figure 6: Fracture properties of CTBN rubber modified bulk epoxy polymers and syntactic foams.

For the syntactic foams, the unmodified foam had a K_{IC} of 0.80 ± 0.03 MPa $m^{1/2}$ and a G_{IC} of 193 ± 12 J/m^2. These values are larger than that of the unmodified bulk epoxy polymer, indicating that the GMS has provided some toughening. From a previous study [7], the main toughening mechanisms identified that were due to the GMS particles were crack deflection, debonding and plastic void growth. The triaxial stresses ahead of the crack tip cause the GMS particles within the plastic zone to debond from the epoxy matrix. This debonding relieves the stress triaxiality at the crack tip, hence allowing the matrix to deform via plastic void growth [36]. Gent [37] describes the debonding process as being dependent on the particle diameter, strength of the particle-to-matrix adhesion, and the modulus of the matrix. When the matrix of the syntactic foams was modified with CTBN, there was no change in K_{IC} and G_{IC} within experimental error at 3 and 6 wt% of CTBN. At higher concentrations, the fracture properties increased slightly, with K_{IC} of 0.94 ± 0.04 MPa $m^{1/2}$ and G_{IC} of 296 ± 26 J/m^2 achieved at 12 wt% CTBN. This corresponds to a 53% increase in fracture energy compared to the unmodified foam. While this improvement is comparable to those seen in the literature [1–6], it is significantly less than that seen for the bulk epoxy polymers.

The fracture energy values, and the change in fracture energy with respect to the unmodified material, ΔG_{IC}, are summarised in Table 1. Full transferability of toughness is achieved if ΔG_{IC} of the syntactic foam is equivalent to $0.4 \times \Delta G_{IC}$ of the bulk epoxy polymer, since 60% of the volume in the foam is occupied by GMS, leaving 40 vol% epoxy remaining. However, the ΔG_{IC} values are much smaller for all CTBN concentrations (see Table 1), therefore there is little transferability of toughness when CTBN modified epoxies are used as the matrix in syntactic foams. The reasons for this will be discussed below.

3.3 Fractography

Scanning electron microscopy (SEM) was used to observe the fracture surfaces of the bulk epoxy polymers and syntactic foams. Images were taken in the plastic zone after the pre-crack to determine the

Table 1: Fracture energy, G_{IC}, and change in fracture energy, ΔG_{IC}, of CTBN modified bulk epoxy polymers and syntactic foams.

CTBN concentration	Bulk epoxy polymer (J/m^2)			Syntactic foam (J/m^2)	
(wt%)	G_{IC}	ΔG_{IC}	$0.4 \times \Delta G_{IC}$	G_{IC}	ΔG_{IC}
Unmodified	101 ± 8	-	-	193 ± 12	-
3	313 ± 39	+212	+84	202 ± 13	+9
6	485 ± 35	+384	+153	173 ± 12	-20
9	762 ± 27	+661	+264	261 ± 24	+68
12	1112 ± 47	+1011	+404	296 ± 26	+103

toughening mechanisms. Note that the direction of crack propagation in all the images is from left to right.

3.3.1 Bulk epoxy polymer

The SEM images of the fracture surfaces of the CTBN modified bulk epoxy polymers are shown in Figure 7. The fracture surfaces of the CTBN rubber modified epoxies are rougher than those of the unmodified epoxy. Micron-sized circular cavities can be observed, indicating that internal cavitation of the rubber particles has occurred. Some cavities are shallow and are lined with CTBN, while the deeper cavities show more obvious signs of rubber particle cavitation and subsequent plastic void growth, which can be seen as holes in the fracture surface. At higher CTBN concentrations, the deep cavities appear to become more sporadic, especially for the 12 wt% CTBN modified epoxy.

The diameters of the voids in the SEM micrographs were measured and compared to the particle sizes measured from the AFM micrographs. The mean radius of the cavities for the 3 and 6 wt% CTBN modified epoxies is 1.2 μm. It is clear that the radius of the cavities is larger than the radius of the particles, which have a mean radius of 0.87 μm. This shows that plastic void growth of the epoxy has occurred after cavitation of the CTBN particles. Cavitation of the rubber particles relieves the triaxial stress state ahead of the crack tip, allowing plastic void growth of the epoxy to occur which absorbs a significant amount of energy and thus increases the fracture energy [35]. Thus, the plastic void growth toughening mechanism has been identified in this study.

3.3.2 Syntactic foam

The fracture surfaces of the CTBN rubber modified syntactic foams were examined using SEM, and the images have been shown previously in Section 3.1.2 (Figures 2 and 3). For the syntactic foams modified with 3 and 6 wt% CTBN, where the rubber particles displayed spherical morphology, no information is available on the initial size of the CTBN particles, since AFM was not possible on the syntactic foam samples. Whether plastic void growth of the epoxy matrix took place due to the cavitation of the rubber particles is therefore unclear. However, from the results of the SENB tests, no improvement in fracture energy compared to the unmodified foam was recorded for these formulations. From this, it can be inferred that no additional plastic deformation of the epoxy matrix has occurred due to the CTBN particles, as this would otherwise lead to an increase in fracture energy since it is a highly energy absorbent mechanism [35]. The reason for the lack of plastic void growth is due to the restricted space between the GMS particles. The ability for the epoxy to deform around the CTBN particles is therefore limited. Voids that are left by the debonding of GMS will also shield nearby rubber particles from undergoing void growth [38]. The size of the interstitial spaces can be increased by using lower volume fractions of GMS, however, this would come with an obvious penalty in density. Alternatively, using GMS particles with larger diameters can also be explored as this will increase the size of the interstitial spaces, allowing more plastic deformation.

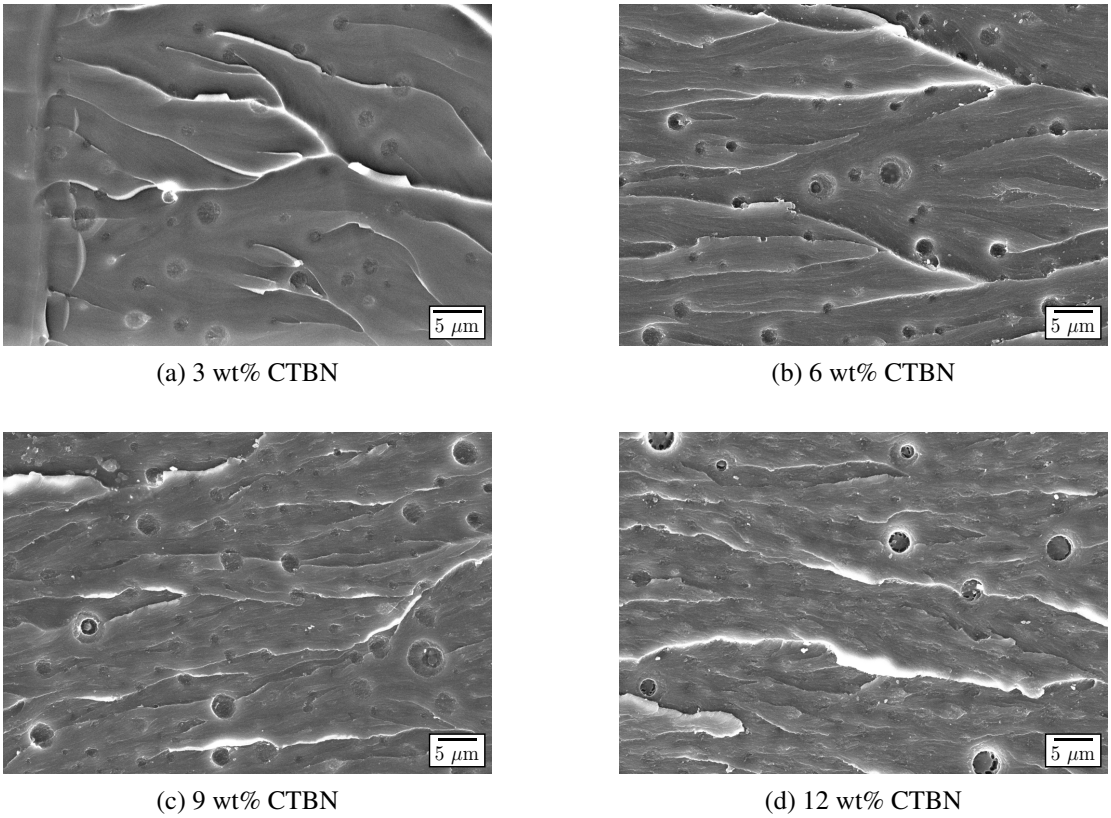

(a) 3 wt% CTBN (b) 6 wt% CTBN

(c) 9 wt% CTBN (d) 12 wt% CTBN

Figure 7: Scanning electron micrographs of the fracture surfaces of CTBN rubber modified bulk epoxy polymers. Crack propagation direction is from left to right.

The syntactic foams modified with 9 and 12 wt% CTBN showed co-continuous rubber morphologies, and these structures may be responsible for the increases in fracture energy observed in these formulations, see Table 1. Co-continuous structures have been found to cause large increases in fracture energy of block copolymer modified epoxies [39, 40], although the toughening mechanisms and the modelling of fracture energy of co-continuous structures are not well understood. Chen and Taylor [39] proposed several mechanisms to explain the large improvements in toughness. In a co-continuous structure, the hard and soft composite-like structure spans across the fracture surface. The soft phase deforms and absorbs energy more readily than the epoxy phase, due to the low yield stress and high ductility of the soft phase. This deformation and energy absorption occurs before the epoxy ligaments spanning across the crack surfaces fracture, effectively blunting the crack tip and leading to large increases in fracture energy [41]. It is proposed that the interconnected structures of rubber and epoxy can interact beyond the interstitial spaces between the hollow glass microspheres, effectively increasing the size of the plastic deformation zone and thus increase toughness.

4 CONCLUSIONS

The microstructure, fracture properties, and toughening mechanisms of bulk epoxy polymer and syntactic foam modified with CTBN were investigated and compared. For the bulk epoxy polymers, the CTBN phase separated into well-dispersed spherical particles for all CTBN concentrations. The CTBN also formed spherical particles in the syntactic foams at lower concentrations (3 and 6 wt%). As the concentration increases, the rubber particles begin to elongate along the surface of the GMS, forming co-continuous and phase inverted structures. The difference in CTBN morphology between the bulk epoxy polymer and syntactic foam was attributed to the reduced dimensionality coupled with particle coalescence in the growth evolution of phase separating CTBN rubber, introduced by the presence of the GMS.

The fracture energy showed a significant increase for the CTBN modified bulk epoxy polymers, from 101 ± 8 J/m^2 to 1112 ± 47 J/m^2 for 12 wt% CTBN. The toughening mechanisms were identified as shear band yielding and plastic void growth after cavitation of the rubber particles.

The fracture energy of the syntactic foams did not increase when the epoxy matrix was modified with 3 and 6 wt% CTBN and remained around 200 J/m^2, but increased gradually to 296 ± 26 J/m^2 at 12 wt%. The co-continuous structures that are present only at these high concentrations are thought to be the cause of the increase in toughness, due to the alternating hard-soft lamellar structure that spans across the fracture surface. However, this increase is much less than that achieved in the bulk epoxy polymer, therefore there is little transferability of toughness. Rubber particles in the syntactic foam have limited space in the interstitial regions between the GMS to undergo plastic void growth, so improvements in fracture energy are limited. Nevertheless, the toughness improvement achieved in this work allows for more lightweight, damage-resistant structures to be produced, increasing the number of applications of syntactic foams in the aerospace and naval industries.

ACKNOWLEDGEMENTS

This work was supported by an EPSRC Industrial CASE studentship funded by the UK Engineering and Physical Sciences Research Council and FAC Technology. Grant number: EP/N509486/1.

REFERENCES

[1] E. M. Wouterson, F. Y. C. Boey, S. -C Wong, L. Chen, and X. Hu. Nano-toughening versus micro-toughening of polymer syntactic foams. *Composites Science and Technology*, 67(14):2924–2933, 2007.

[2] A. Asif, V. Lakshmana Rao, and K. N. Ninan. Nanoclay reinforced thermoplastic toughened epoxy hybrid syntactic foam: Surface morphology, mechanical and thermo mechanical properties. *Materials Science and Engineering: A*, 572:6184–6192, 2010.

[3] E. Zegeye, A. K. Ghamsari, and E. Woldesenbet. Mechanical properties of graphene platelets reinforced syntactic foams. *Composites Part B: Engineering*, 60:268–273, 2014.

[4] R. Ciardiello, L. T. Drzal, and G. Belingardi. Effects of carbon black and graphene nano-platelet fillers on the mechanical properties of syntactic foam. *Composite Structures*, 178:9–19, 2017.

[5] L. Zhang and J. Ma. Effect of carbon nanofiber reinforcement on mechanical properties of syntactic foam. *Materials Science and Engineering: A*, 574:191–196, 2013.

[6] K. R. Dando and D. R. Salem. The effect of nano-additive reinforcements on thermoplastic microballoon epoxy syntactic foam mechanical properties. *Journal of Composite Materials*, 52(7):971–980, 2018.

[7] S. He, D. Carolan, A. Fergusson, and A. C. Taylor. Toughening epoxy syntactic foams with milled carbon fibres: Mechanical properties and toughening mechanisms. *Materials & Design*, 169:107654, 2019.

[8] E. M. Wouterson, F. Y. C. Boey, X. Hu, and S. Wong. Effect of fiber reinforcement on the tensile, fracture and thermal properties of syntactic foam. *Polymer*, 48(11):3183–3191, 2007.

[9] C. Huang, Z. Huang, Y. Qin, J. Ding, and X. Lv. Mechanical and dynamic mechanical properties of epoxy syntactic foams reinforced by short carbon fiber. *Polymer Composites*, 37(7):1960–1970, 2016.

[10] J. N. Sultan and F. J. McGarry. Effect of rubber particle size on deformation mechanisms in glassy epoxy. *Fatigue and Fracture of Engineering Materials and Structures*, 13(1):29–34, 1973.

[11] J. W. Cahn and J. E. Hilliard. Free energy of a nonuniform system. I. Interfacial free energy. *The Journal of Chemical Physics*, 28(2):258–267, 1958.

[12] D. Carolan, H. M. Chong, A. Ivankovic, A. J. Kinloch, and A. C. Taylor. Co-continuous polymer systems: A numerical investigation. *Computational Materials Science*, 98:24–33, 2015.

[13] R. Bagheri, B. T. Marouf, and R. A. Pearson. Rubber-toughened epoxies: A critical review. *Journal of Macromolecular Science, Part C: Polymer Reviews*, 49(3):201–225, 2009.

[14] Evonik. *Technical data sheet Albipox 1000*. Evonik, Germany, 2014.
[15] Huntsman Advanced Materials. *Technical data sheet of Araldite LY 556 / Aradur HY 917 / Accelerator DY 070*. Huntsman Corporation, Switzerland, 2007.
[16] G. Giannakopoulos, K. Masania, and A. C. Taylor. Toughening of epoxy using core-shell particles. *Journal of Materials Science*, 46:327–338, 2011.
[17] S. C. Kunz, J. A. Sayre, and R. A. Assink. Morphology and toughness characterization of epoxy resins modified with amine and carboxyl terminated rubbers. *Polymer*, 23(13):1897–1906, 1982.
[18] T. -H. Hsieh, A. J. Kinloch, K. Masania, J. Sohn Lee, A. C. Taylor, and S. Sprenger. The toughness of epoxy polymers and fibre composites modified with rubber microparticles and silica nanoparticles. *Journal of Materials Science*, 45(5):1193–1210, 2010.
[19] 3M. *Technical data sheet of 3M Glass Bubbles S38*. 3M, USA, 2010.
[20] ISO 13586. *Plastics - Determination of fracture toughness (G_{IC} and K_{IC}) - Linear elastic fracture mechanics (LEFM) approach*. International Organization for Standardization, Geneva, Switzerland, 2018.
[21] A. J. Kinloch and D. L. Hunston. Effect of volume fraction of dispersed rubbery phase on the toughness of rubber-toughened epoxy polymers. *Journal of Materials Science Letters*, 6(2):137–139, 1987.
[22] E. E. Underwood. *Quantitative stereology*. Addison-Wesley Pub. Co., Reading, USA, 1970.
[23] K. Yamanaka and T. Inoue. Phase separation mechanism of rubber-modified epoxy. *Journal of Materials Science*, 25(1):241–245, 1990.
[24] J. -P. Chen and Y. -D. Lee. A real-time study of the phase-separation process during polymerization of rubber-modified epoxy. *Polymer*, 36(1):55–65, 1995.
[25] D. Carolan, A. Ivankovic, A. J. Kinloch, S. Sprenger, and A. C. Taylor. Toughening of epoxy-based hybrid nanocomposites. *Polymer*, 97:179–190, 2016.
[26] I. McEwan, R. A. Pethrick, and S. J. Shaw. Water absorption in a rubber-modified epoxy resin; carboxy terminated butadiene acrylonitrile-amine cured epoxy resin system. *Polymer*, 40(15):4213–4222, 1999.
[27] G. Tripathi and D. Srivastave. Effect of carboxyl-terminated poly(butadiene-co-acrylonitrile) (CTBN) concentration on thermal and mechanical properties of binary blends of diglycidyl ether of bisphenol-A (DGEBA) epoxy resin. *Materials Science and Engineering: A*, 443(1-2):262–269, 2007.
[28] P. Wiltzius and A. Cumming. Domain growth and wetting in polymer mixtures. *Physical Review Letters*, 66(23):3000–3003, 1991.
[29] A. Cumming, P. Wiltzius, F. S. Bates, and J. H. Rosedale. Light-scattering experiments on phase-separation dynamics in binary fluid mixtures. *Physical Review A*, 45(2):885–897, 1992.
[30] M. L. Hair. Hydroxyl groups on silica surface. *Journal of Non-Crystalline Solids*, 19:299–309, 1975.
[31] E. H. Andrews, He Pingsheng, and C. Vlachos. Adhesion of epoxy resin to glass. *Proceedings of the Royal Society of London A: Mathematical, Physical and Engineering Sciences*, 381(1781):345–360, 1982.
[32] S. M. Troian. Coalescence induced domain growth near a wall during spinodal decomposition. *Physical Review Letters*, 71(9):1399–1402, 1993.
[33] F. E. Torres and S. M. Troian. Diffusive growth of phase-separating domains near a surface: the effect of reduced dimensionality. *Colloids and Surfaces*, 89(2-3):227–239, 1994.
[34] T. M. Rogers, K. R. Elder, and R. C. Desai. Droplet grwoth and coarsening during heterogeneous vapor condensation. *Physical Review A*, 38(10):5303–5309, 1988.
[35] Y. Huang and A. J. Kinloch. Modelling of the toughening mechanisms in rubber-modified epoxy polymers - Part II. A quantitative description of the microstructure-fracture property relationships. *Journal of Materials Science*, 27(10):2763–2769, 1992.
[36] A. F. Yee, D. Li, and X. Li. The importance of constraint relief caused by rubber cavitation in the

toughening of epoxy. *Journal of Materials Science*, 28:6392–6398, 1993.

[37] A. N. Gent. Detachment of an elastic matrix from a rigid spherical inclusion. *Journal of Materials Science*, 15(11):2884–2888, 1980.

[38] D. J. Bray, P. Dittanet, F. J. Guild, A. J. Kinloch, K. Masania, R. A Pearson, and A. C. Taylor. The modelling of the toughening of epoxy polymers via silica nanoparticles: The effects of volume fraction and particle size. *Polymer*, 54(26):7022–7032, 2013.

[39] J. Chen and A. C. Taylor. Epoxy modified with triblock copolymers: morphology, mechanical properties and fracture mechanisms. *Journal of Materials Science*, 47(11):4546–4560, 2012.

[40] A. Klinger, A. Bajpai, and B. Wetzel. The effect of block copolymer and core-shell rubber hybrid toughening on morphology and fracture of epoxy-based fibre reinforced composites. *Engineering Fracture Mechanics*, 203:81–101, 2018.

[41] H. M. Chong and A. C. Taylor. The microstructure and fracture performance of styrene-butadiene-methylmethacrylate block copolymer-modified epoxy polymers. *Journal of Materials Science*, 48(19):6762–6777, 2013.